JOURNAL OF GEOPHYSICAL RESEARCH, VOL. 96, NO. C4, PAGES 6951–6963, APRIL 15, 1991

A Zonal-Averaged Model of the Ocean's Response to Climatic Change

STEFAN RAHMSTORF[1]

Research School of Earth Sciences, Victoria University, Wellington, New Zealand

A new vertical mixing model is described. It combines a box-advection-diffusion model with a bulk mixed layer model, which simulates wind mixing and penetrative convection. It is shown that mixed layer models can have steady periodic solutions if either the mixing decays to zero at depth or vertical advection is included. The latter approach is adopted. This mixing model is applied to a series of latitude bands between 50°N and 50°S. It successfully simulates present-day seasonal cycles of temperature and mixed layer depth. It is then subjected to an additional heat flux resulting from an increase in greenhouse gases. For an equilibrium warming of 3°C for CO_2 doubling, the model predicts the following transient response: a 0.5-0.8°C temperature rise from 1850 to 1990, and a 1.5-2.0°C rise from 1850 to 2050. The ocean acts as a thermal buffer, so that the actual warming lags the equilibrium warming by 25-50 years. Mixed layer and deep ocean contribute about equally to this lag. The seasonal cycle of mixed layer depth pumps more heat down to deeper waters, compared to a fixed mixed layer depth model. The heat uptake depends strongly on possible changes in the global thermohaline circulation, which could therefore affect sea level predictions. The climatic warming also leads to a reduction in winter mixing depth in the higher latitudes, whereas the mixing depth in other seasons and latitudes would be mainly affected by wind changes. A scenario for reduced CO_2 emissions shows that the surface warming can be slowed dramatically but that a long-term sea level rise from thermal expansion may be inevitable.

1. INTRODUCTION

As evidence is mounting that the human species is disturbing the climatic balance of the Earth, efforts to improve our understanding of this balance have become more urgent. It has become clear that the oceans play a crucial role in the climate system of our home planet. This role is still not very well understood. The representation of ocean physics seems to be a weak point in the models that attempt to predict the future development of our climate.

It is generally expected that the vast heat capacity of the oceans will delay the thermal response to a change in external forcing, such as the greenhouse effect. The important question is: how will the thermal structure of the oceans change in space and time for a given change in surface forcing? The key to this question is mixing. If the oceans were mixed from top to bottom, they could take up a large amount of extra heat with only a small increase in surface temperature, and their response time to any heating changes would be long, of the order of 150 years [*Hoffert et al.*, 1980]. If on the other hand the mixing were confined to a thin surface layer, then only the heat capacity of this layer would be accessible to store extra heat, and the response time would be much shorter (about 5 years for 100 m layer thickness). The real ocean is of course more complex than these two examples. There is a well-mixed surface layer, the depth of which varies in space and time, below which limited mixing occurs. Water motions on all scales contribute to the redistribution of heat in the ocean, from microturbulence to global circulation patterns. We need a model that simulates the climatically important heat transport mechanisms in the ocean.

Several such models have been published. We focus on one-dimensional models here, as we are interested in vertical mixing processes. These are probably the most important in determining sea surface temperatures, and a model of vertical mixing can of course later be included as a process model into a more comprehensive three-dimensional simulation. At this stage, most of the published models for the role of the oceans in climatic change are essentially one-dimensional.

In these models the ocean is treated as one or more isothermal boxes with a given rate of heat transfer between them or as a water column with a vertical temperature gradient, where turbulent diffusion and upwelling act as heat transport mechanisms. *Schneider and Thompson* [1981] discuss models that consist of a single box either of mixed layer depth (about 100 m), or of the average total ocean depth (about 4000 m), and compare them to a two-box model with a mixed layer box overlying a deep ocean box. In a similar approach, *Harvey and Schneider* [1985] use three boxes: an equivalent mixed layer, an intermediate layer, and a bottom layer. Often an isothermal surface mixed layer of fixed thickness is combined with a diffusive, or advective-diffusive, deep ocean [*Hoffert et al.*, 1980; *Cess and Goldenberg*, 1981; *Wigley and Schlesinger*, 1985; *Harvey and Schneider*, 1985; *Wigley and Raper*, 1987].

Although the results of these models are not very sensitive to the choice of mixed layer depth (typically 100 m), *Henderson-Sellers* [1988] concludes that fixed mixed layer depth models are inadequate. Prognostic mixed layer models, which predict mixed layer depth and therefore allow for seasonal and long-term changes, have also been applied to the CO_2 problem [*Hunt and Wells*, 1979], but in this case the heat storage below the mixed layer was neglected. *Henderson-Sellers* [1987] used a

[1]Now at New Zealand Oceanographic Institute, DSIR, Wellington.

Paper number 90JC02738.
0148-0227/91/90JC-02738$05.00

convection-diffusion model with a wind- and depth-dependent eddy diffusivity to simulate oceanic temperature changes, but this model too was limited to the near-surface layer.

The general picture given by the models is that the deep ocean delays the temperature response to the greenhouse forcing currently by about two or three decades. Present warming should be about half the equilibrium warming for present CO_2 levels. Predictions of the warming to today vary according to the assumptions made but are generally not inconsistent with the observed warming of 0.5 °C over the past 100 years [*Jones et al.*, 1986]. The exception is the *Henderson-Sellers* [1987] model, which predicts a much smaller temperature increase.

More specific aspects of some of these models will be discussed later. In this paper, we propose a model that draws upon ideas of all the models mentioned above and includes them in a more detailed view of the ocean's thermal stratification. To simulate near-surface wind mixing and convection, we use an improved, fully prognostic integral mixed layer model. This is coupled to an advective-diffusive deep ocean. The details of this model are described below. It is applied to different latitude bands and run to equilibrium, representing today's global ocean temperatures. The model is then subjected to a change in surface forcing simulating the greenhouse effect.

2. A FOUR-PROCESS MODEL FOR THERMAL STRATIFICATION

The model that we describe in this section aims to simulate four physical processes that redistribute heat vertically in the water column. These are wind mixing, convection, upwelling, and turbulent diffusion below the mixed layer.

As shown in Figure 1, the model basically consists of an isothermal mixed layer coupled to a thermocline deep ocean. The main difference to similar models [e.g., *Harvey and Schneider*, 1985] is that the mixed layer depth is not prescribed but depth and temperature of the mixed layer are calculated from integrated kinetic and thermal energy budgets. Therefore the mixed layer runs through a realistic seasonal cycle. It responds to winter cooling with penetrative convection, to excessive wind mixing with entrainment, etc. The model will also predict changes in mixed layer depth resulting from the greenhouse warming.

It should be noted here that this simple model does not attempt to make a prediction of greenhouse warming. Rather it investigates certain aspects of this warming, assuming that the warming occurs. Specifically, the model tries to clarify the role of the oceanic mixed layer and its seasonal cycles in climatic change. A bulk mixed layer model like the one used here is being built into the Hamburg ocean general circulation model (E. Maier-Reimer, personal communication, 1990) for the purpose of climate predictions. The simple scheme used in this paper has the advantage of isolating the vertical mixing processes, thereby allowing us to understand better their physical significance for the climate problem.

2.1. *Energy Budget of the Mixed Layer*

The approach used in this paper to model the mixed layer was pioneered by *Kraus and Turner* [1967]. The two

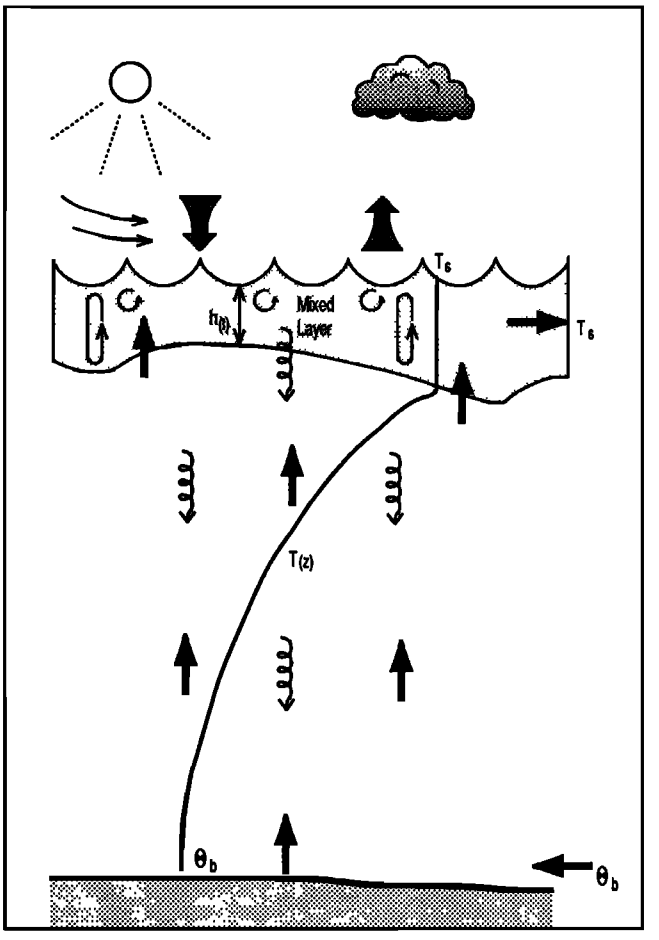

Fig. 1. The model includes a mixed layer (shaded) of depth $h(t)$ and temperature $T_s(t)$. At the surface, heat is exchanged and the wind blows. Within the mixed layer, wind mixing and convection act to stir the water. Heat is diffused downward into the deep ocean below. Near the ocean bottom, cold water of temperature θ_b enters. It is advected upward and leaves the mixed layer at temperature T_s.

independent parameters, mixed layer depth h and temperature T, are determined by the heat conservation equation

$$h\frac{dT}{dt} + \Delta T w_e = -\frac{1}{c_p \rho_0} Q \qquad (1)$$

and the mechanical energy equation

$$-\frac{g}{2\rho_0} h \Delta\rho w_e = mU^3 - \frac{1}{2} nhB \qquad (2)$$

The surface buoyancy flux is $B = (g\alpha/c_p\rho_0)Q$, where Q is the surface heat flux, α is the thermal expansion coefficient, and c_p is the heat capacity of seawater. For the purpose of this paper we ignore the effect of salinity on the buoyancy flux. Together with an equation of state $\rho(T)$ the system is closed and allows us to calculate $h(T)$ and $T(t)$ for a given heat flux $Q(t)$ and wind speed $U(t)$. For a derivation of these equations, see, for example, *Niiler and*

Kraus [1977]. The entrainment velocity w_e is defined as

$$w_e = \begin{cases} dh/dt & dh/dt > 0 \\ 0 & dh/dt \le 0 \end{cases}$$

The first term of (2) is the amount of energy needed to deepen the mixed layer by entraining denser water from below, with a density step $\Delta\rho$ at the mixed layer base. The second term is the turbulent energy from the wind that is used to increase the potential energy. This is only a small fraction of the total wind power; the factor m is empirical. The last term is the buoyancy term. If B is positive (heating), $n = 1$ and $hB/2$ is the work against buoyancy that is required to keep the mixed layer mixed while it warms. If B is negative (cooling), potential energy is released, a fraction f of which can be used for further entrainment. The way we have written it here

$$n = \begin{cases} 1 & B > 0 \\ f & B < 0 \end{cases}$$

The case $f = 0$, where none of the convective energy enters the budget (2) is called nonpenetrative convection.

If we introduce B and ρ into (1), and subtract (2), we obtain

$$\frac{g}{2\rho_0} h^2 \frac{d\rho}{dt} + \frac{g}{\rho_0} h \Delta\rho w_e = -mU^3 - \frac{1-n}{2} hB \qquad (3)$$

The left-hand side can be interpreted as the rate of change of potential energy in the water column, $-(1/\rho_0)\,(dE_{pot}/dt)$. Then mU^3 is the wind input to the potential energy of the water column, and for $B<0$ (cooling), $-(1-f)hB/2$ is the rate of decrease of potential energy due to dissipation of convective energy.

2.2. *Periodic Solutions*

We now have the tools to answer a question that is important for longterm climate modelling: can this type of mixed layer model have a steady periodic solution? *Gill and Turner* [1976] have pointed to the problem that the potential energy in this model type tends to increase from one year to the next. From (3) we see that for fully penetrative convection, $f = 1$, the last term vanishes and the potential energy increases monotonically. For $f < 1$, a fraction $(1-f)$ of the convective energy is dissipated, leading to a decrease of potential energy. However, part is reinvested, and it can be shown that only if $f = 0$ at the time of maximum h can we dissipate enough energy during the cooling season to obtain a closed seasonal cycle.

The same holds for the wind efficiency parameter m. For a cyclical solution, h_{max} must coincide with the end of the cooling season $B = 0$, otherwise potential energy would be stored below the depth of deepest convection. This would be irreversible. For entrainment to stop at $B=0$, mU^3 must vanish in (2) so that w_e can go to zero. We therefore conclude that when the maximum mixed layer depth is reached, both wind and convective mixing must stop if a periodic solution is to be obtained.

This is how previous authors have constructed mixed layer models with cyclical solutions. They made m and f a function of h, so that they vanish when h gets too large [e.g., *Garwood*, 1977; *Hunt and Wells*, 1979; *Woods and Barkmann*, 1986; *Gaspar*, 1988.] Although this may be plausible for the wind efficiency m, there is no physical reason why the turbulence generated by convection should not be available at the mixed layer base. It originates throughout the mixed layer, not near the surface like the wind mixing. The assumption that f goes to zero with increasing h is therefore unphysical.

At this point we should stress that this problem is in no way peculiar to bulk mixed layer models: it is a property of all mixing models, simply following from the second law of thermodynamics. *Henderson-Sellers'* [1987] eddy diffusion model avoids it in exactly the same way as bulk models: by using nonpenetrative convection and an eddy diffusivity K that goes to zero at depth. Stratification can only be maintained in the long term if there is either no mixing or if there is a process that opposes the mixing and maintains the gradient. This process is advection. While most mixed layer modellers have chosen the "no-mixing" option, the classical way to model deep ocean stratification has been to introduce a vertical velocity w to balance the downward diffusion [*Munk*, 1966]. We have included the same process in our mixed layer model to give periodic solutions.

Note, however, that the inclusion of a vertical velocity is not strictly a one-dimensional concept. It only makes sense as part of a global thermohaline circulation, with cold dense water sinking in polar areas and with horizontal transport of cold water near the sea bottom and warm water near the surface. *Harvey and Schneider* [1985] discuss this idea in more detail for their model. It means that a small amount of heat is advected out of the model water column, corresponding to a net surface heat gain and poleward heat flux.

2.3. *Coupling to the Deep Ocean*

The mixed layer model described above is embedded into an upwelling-diffusion model of the entire water column, described by

$$\frac{\partial T}{\partial t} = K\frac{\partial^2 T}{\partial z^2} - w\frac{\partial T}{\partial z} \qquad (4)$$

where K is the turbulent diffusion coefficient, w is the vertical velocity, and $T(z)$ is the ocean temperature at depth z. Inside the mixed layer, this parameterization has no effect, as $\partial T/\partial z$ vanishes. The mixed layer base, however, is advected upward with velocity w, leading to a cyclical steady state as discussed above. The sharp temperature step that develops there during the mixed layer deepening is smoothed by the diffusion term. In the deep ocean, (4) leads to the usual balance of advection and diffusion, with an exponential $T(z)$ as steady state solution. Although more modern theories of thermocline ventilation suggest that a more complex, three-dimensional flow pattern maintains the temperature gradient [*Luyten et al.*, 1983], here we limit ourselves to a vertical flow because of the essentially one-dimensional nature of our model.

2.4. *Numerical Implementation*

The model was implemented on a finite difference grid, with 2-m vertical resolution in the top 250 m (to satisfy the requirements of the mixed layer model) and 30 m in the rest of the water column, down to the bottom at 4000 m. Doubling this resolution does not change the results. The time step is 1 day, except for the diffusion in the top 250 m, which is done in a number of shorter steps to satisfy the Courant-Friedrichs-Levy criterion for numerical stability.

At each time step, the following procedure is carried out. First, the heat exchange at the surface is calculated from bulk parameterization formulae for incident shortwave radiation, longwave radiation, latent heat, and sensible heat flux. In order to do this, we need meteorological data about cloud cover, wind speed, air temperature, and humidity. Solar radiation is distributed with depth according to a double exponential law for water type IA [*Paulson and Simpson,* 1977]. After the heat input, the density profile is calculated with a thermal expansion coefficient corresponding to the previous day's temperatures. (This is to avoid unrealistic nonlinear effects from the high near-surface temperatures in the model water column that can occur before the mixing step, at all other stages of the program a density polynomial is used.) Next, a subroutine performs the convective mixing in case an instability has arisen from surface cooling. After that, wind mixing is carried out according to the energy constraints described above. The diffusive changes to the thermal structure are then calculated, where necessary in several sub-time steps. Finally, upward advection is performed. During all this, the program keeps track of the heat flows associated with the different processes, and at the end of each year a detailed heat budget is calculated.

3. BOUNDARY CONDITIONS

In this section we discuss the surface forcing used for our climate simulations, as well as the inflow of cold bottom water from below.

3.1. *Heat Exchange With the Atmosphere*

Four heat exchange terms act at the upper boundary of our model water column: shortwave and longwave radiation and sensible and latent heat flux. How will these be modified by the increase of greenhouse gases in the atmosphere? The greenhouse effect works in two ways at the ocean surface: first, by directly adding to the incoming longwave radiation and, second, by heating the troposphere overlying the ocean. To properly model the effect this has on the sensible and latent heat exchange between atmosphere and ocean, it would be necessary to couple an atmospheric model to the ocean model.

Luckily, however, two facts allow us to estimate the heat exchange at the ocean surface from simple assumptions: the atmosphere's heat capacity is negligible compared to the ocean's, and the atmosphere is in very sensitive thermal contact with the ocean.

The first fact means that for our purposes the atmosphere is always in thermal equilibrium: the fluxes into it add to zero; there is no significant storage term. If the amount of longwave radiation absorbed by the lower troposphere is increased, the lower troposphere will heat up until an increase in the outgoing fluxes cancels the extra incoming flux. The outgoing fluxes are longwave emission to space and exchanges with the ocean. If we look at the sensitivity of these fluxes to an increase in air temperature, we can see how they will change when the atmosphere is warmed. We find that for a 1° increase in tropospheric temperature, the sensible heat flux will change by about 10 W/m^2 and the evaporative heat flux by 15 W/m^2 (depending on humidity and wind speed), both in the direction of extra heat flux into the ocean. In comparison, the extra radiation to space will increase only by about 2 W/m^2. This and the fast temperature response of the troposphere mean that it will pass most of the greenhouse heat flux it absorbs directly on to the ocean. The ocean thus receives nearly all of the extra greenhouse flux that heats the surface-troposphere system, either directly or via the troposphere. The ocean cannot redress this imbalance by giving off heat to the atmosphere; it must heat up until back radiation to space cancels the extra incoming flux.

The appropriate upper boundary condition for our model ocean is arrived at, therefore, by adding the amount of greenhouse heating received by the surface-troposphere system to the ocean's surface heat budget. The back radiation term is allowed to increase as the ocean warms, whereas the sensible and latent heat fluxes are held at their pregreenhouse equilibrium levels.

With this assumption we obtain an equilibrium warming of the ocean surface of 3°C, for a 4 W/m^2 greenhouse radiation (CO_2 doubling). It should be clear that this is not a new prediction of greenhouse warming, as the model contains no atmosphere but relies on heating predictions of an atmospheric model [*Ramanathan et al.,* 1979] and the approximations explained above. Rather, we have a process model that looks at oceanic heat uptake and how this modifies the warming. It is suitable to be used as a building block in a more comprehensive model of the ocean-atmosphere system, which would then have a capacity to make stand-alone predictions of greenhouse warming.

Note that the boundary condition we derived here is different from one that assumes a constant air-sea temperature difference ΔT_{ao} during a warming climate. With our parameterizations, a constant ΔT_{ao} at increasing temperatures would lead to an increase of the evaporative heat flux to the atmosphere, and the ocean would just leak most of the extra heat to an "infinite sink" atmosphere through the evaporation term. This is unphysical, as discussed above. During the transient response to climatic warming, the atmosphere warms faster, and the heat flux from the ocean to the atmosphere has to be reduced. This is associated with a reduction of ΔT_{ao}. The thermal inertia of the ocean will nevertheless slow down the warming of the atmosphere, because the change in ΔT_{ao} will only be small.

Note also that our boundary condition does not allow for any extra atmospheric heat accumulated over the continents being transported toward the oceans. This corresponds to a "no-wind" limit for horizontal transfer in the atmosphere [*Thompson and Schneider,* 1979, Appendix A]. Therefore, our results will be more accurate in the southern hemisphere. In the northern hemisphere the effects of continents could lead to extra heating and a faster ocean temperature rise. The results of *Cess and*

Goldenberg [1981] suggest, however, that this effect is small.

3.2. *Thermohaline Circulation*

As mentioned before, once a vertical velocity w is included, the model is not strictly one-dimensional; this upwelling has to be seen as part of a global thermohaline circulation pattern. Cold water sinks in confined polar regions and spreads along the seafloor to feed the slow upwelling in the rest of the ocean. To close the cycle, water has to flow back toward the poles near the surface. Because this near-surface water is warmer than the equatorward flowing bottom water, this circulation is a simple mechanism for poleward heat transport. This thermohaline circulation has been taken into account in some of the published one-dimensional climate models, and is discussed more fully there [*Hoffert et al.*, 1980; *Harvey and Schneider*, 1985]. Following Hoffert et al. we use an upwelling velocity of 4 m/yr throughout. This is balanced by downward diffusion, allowing a steady state temperature gradient in the ocean.

There are two aspects of this thermohaline circulation that should be discussed in more detail. The first is the temperature of the bottom water, θ_b. This water enters our model water column from below, and its temperature must be specified as a bottom boundary condition. *Hoffert et al.* [1980] use 1.2°C for present-day conditions, and they assume that θ_b will increase as the sea surface temperature in the polar regions warms up. They define a polar sea warming parameter Π as the ratio of the polar sea surface temperature increase to the mixed layer temperature increase and perform their calculations for a range of Π values. For example, if the polar seas warm up twice as fast as the average mixed layer temperature, then $\Pi = 2$. The bottom water fed in at the lower boundary then gets progressively warmer, heating the water column from below. Not surprisingly, the choice of Π has a dramatic effect on their simulation results, especially for the deep ocean temperature.

In our view, it is unlikely that this warmer polar water could sink to the bottom to heat the world ocean at depth. Rather, it would sink less deep so that progressively the deeper parts of the ocean are cut off from the thermohaline circulation, or this circulation is weakened altogether. The latter view is consistent with model results of *Bryan et al.* [1988], where the weakening of the circulation delays the warming of the southern ocean. *Harvey and Schneider* [1985] argue that the rate of bottom water formation in the Weddell Sea would decrease in a warming climate but the temperature of this water would remain unchanged, as it is tightly constrained by the physics of the formation process. This would mean that θ_b remains constant but w decreases. To assess the possible effect of this on our model, we did a test run for decreasing w.

The second important aspect of the thermohaline circulation is the poleward heat transport associated with it. In our model water column, warm water is removed from the surface mixed layer as cold water enters from below. The vertical advection thus leads to a net heat loss throughout the water column. *Harvey and Schneider* [1985] prevent this heat loss by removing the advected water from the mixed layer at the temperature θ_b, although of course there is no such cold water near the surface. This technique conserves heat during the advection process, by heating the mixed layer by the same amount as the water below it is cooled. It leads to artefacts like an overshooting of the surface temperature over the equilibrium warming in some of their simulations.

In this paper, we take a different approach. We allow a net advective heat loss to happen, as part of the thermohaline circulation. In equilibrium, this is automatically balanced by a net surface heat gain. To conserve heat on a global scale, we assume that the regions of polar bottom water formation are areas of net surface cooling, so that the heat gain in the rest of the ocean is cancelled. This is fully consistent with the concept of the thermohaline circulation.

We will apply our model to latitude bands, and Figure 2 illustrates the heat flow in this case. The heat advected out of one latitude zone is simply added to the zones closer to the pole. We do this by starting our numerical simulations at the equator and storing daily values of mixed layer temperature. We can then work out the heat flux into each zone from the temperature difference to the neighbouring (equatorward) zone and from continuity. The poleward heat flux obtained in this way is 2.4×10^{14} W across 5°N and 5°S. It peaks at mid-latitudes (11.2 and 11.0×10^{14} W at 35°N and 35°S, respectively), and is 5.7×10^{14} W across 55°N and 5.0×10^{14} W across 55°S. These values are consistent with observed oceanic heat transport values (reviewed by *Hsiung* [1985]), considering that the thermohaline circulation accounts only for part of the total poleward heat flux. The meridional heat flux in the atmosphere is implicitly included in the model through the use of observed atmospheric temperatures.

The described procedure ensures global heat conservation in the model. It cannot model changes in meridional heat transport that may accompany climate change, however. To do this, one would need a three-dimensional coupled ocean-atmosphere circulation model. The scenarios presented here show a nearly uniform

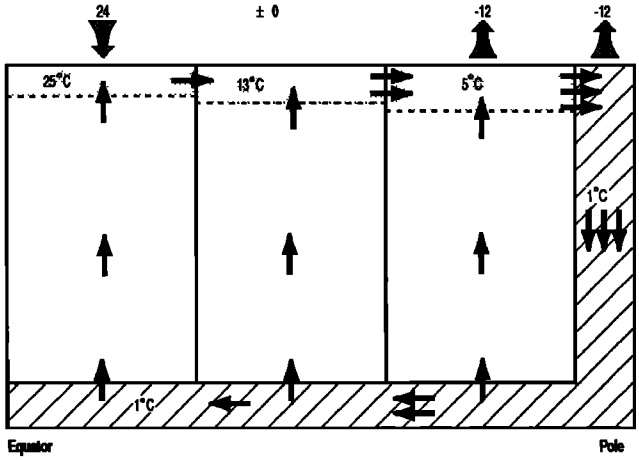

Fig. 2. A simple schematic example of heat conservation with three water columns. Cold water sinks near the pole and is fed into the model water columns from below. In the equator column, water enters at 1°C and leaves the mixed layer at 25°C, a net loss of 24 "temperature units". This loss is balanced by an equal net surface gain. The second column loses 12 units (13° - 1°) from the vertical flow, but gains 12 units (25° - 13°) from horizontal advection, and so on. The total surface balance for the globe is closed by an assumed net heat loss over the polar sinking areas.

warming across all model latitudes, in which case we do not expect major changes in the meridional distribution of heat. An exception is a scenario with a reduction in the thermohaline circulation, which will be discussed in section 5.3.

4. VALIDATION AND TUNING OF THE MODEL

To validate the model for the present climate, it was forced with long-term average climate data for different latitude bands, ranging from 50°S to 50°N. The climatic data were obtained from the Marine Climatological Atlas of the World [*U.S. Navy*, 1981]. The model was run until a cyclical steady state was reached. In principle, we can start from arbitrary initial conditions, but because of the slow response of the deep ocean it could take a thousand years to reach the equilibrium profile. Of course, we already know that the steady state solution for the deep ocean is an exponential function. Through a process of guessing a suitable sea surface temperature, we can speed up the approach to equilibrium by starting very close to the steady state profile. This procedure enabled us to restrict our equilibrium simulations to 200 years duration.

The annual sea surface temperature cycles obtained by the model are shown in Figure 3 and compared to monthly data from the Marine Climatological Atlas. The agreement is very good except at the equator, which is about 1°C too warm in the model. This is perhaps due to cooling by local upwelling near the equator, a process not included in our model.

The good agreement of surface temperatures shows that the surface heat exchange feedbacks were modelled successfully. It is not, however, a critical test of the vertical mixing in the model. To assess whether vertical mixing is modelled well, we have to look at the annual cycle of mixed layer depth. Figure 4 shows a contour plot of this, for the northern hemisphere. The main features agree well with observations. In the equatorial region, the mixed layer depth is around 60 m throughout the year. In higher latitudes, the seasonal cycle is more pronounced. At 50°N, the mixed layer is less then 20 m thick in summer but reaches 180 m depth in winter. (Contours below 100 m are not shown in Figure 4, because the observational data extend only to this depth.)

The wind mixing efficiency m in the model was adjusted to fit these observations. As mentioned in section 2.2, this efficiency decreases with increasing mixed layer depth h. The value we have used throughout is

$$m = 0.4\times10^{-3} \exp(-h/50\text{ m})\, \rho_a\, \kappa, \qquad (5)$$

where ρ_a is the air density (1.2 kg/m^3) and κ is the drag coefficient (1.2×10^{-3}). This is smaller than the value of $1.2\times10^{-3} \exp(-h/100\text{ m})\, \rho_a\, \kappa$ that *Woods and Barkmann* [1986] fitted for a location in the North Atlantic. The difference is plausible for two reasons. They used a 1-hour time step, compared to one day in this work. If the diurnal cycle is resolved, a larger m is required, due to nonlinearities. The second reason is the eddy diffusion

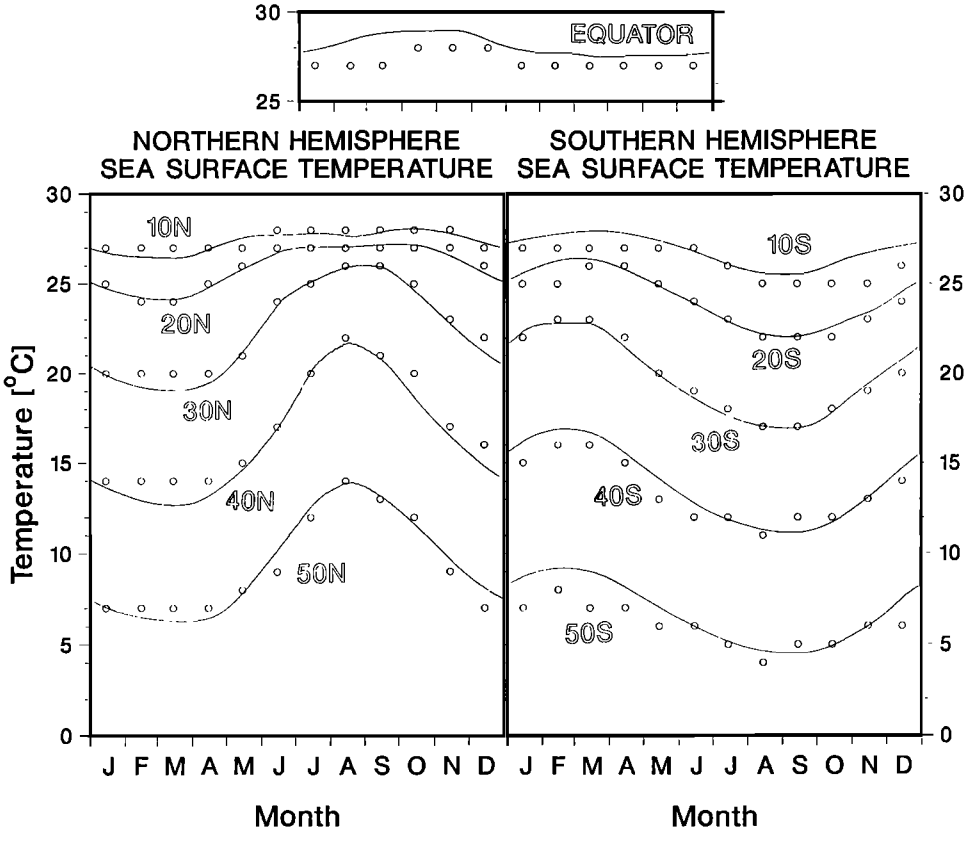

Fig. 3. A comparison of model sea surface temperatures (curves) with monthly mean observations for different latitudes. The observations were zonally averaged by eye from atlas charts and are only estimated to the nearest degree Celsius.

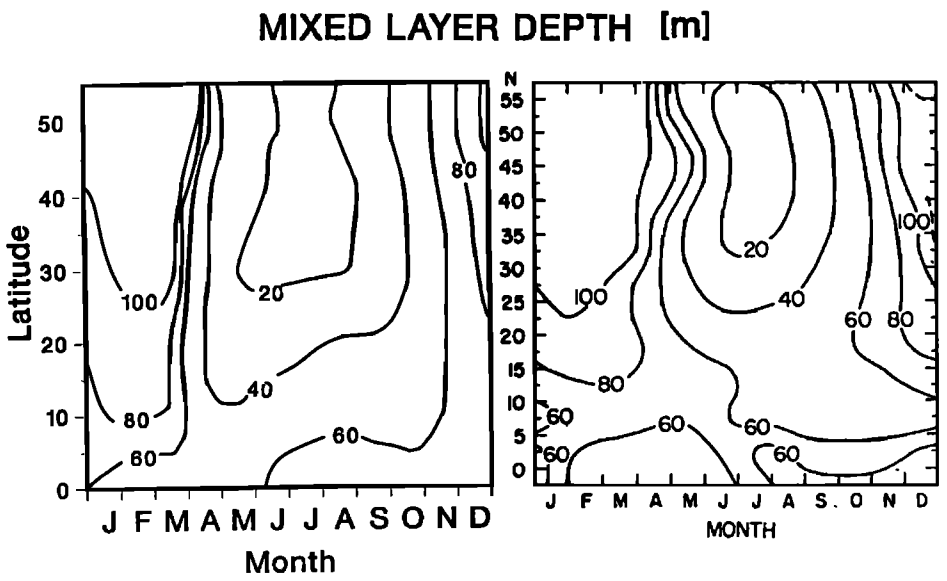

Fig. 4. The annual cycle of zonal mean mixed layer depth for the northern hemisphere. (Left) model results and (right) observations after *Meehl* [1984].

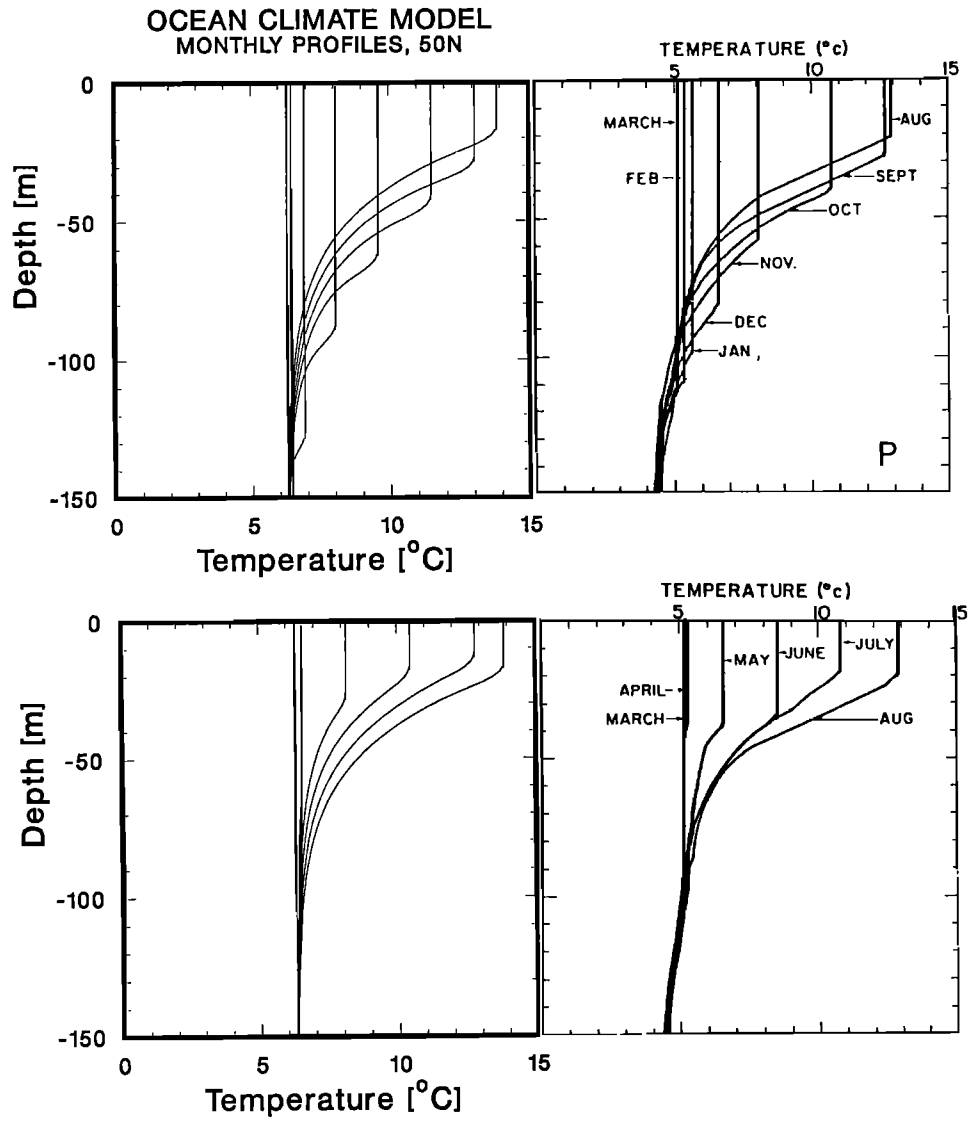

Fig. 5. (Right) monthly temperature profiles from OWS Papa (long-term average after *Tabata* [1976]) and (left) model profiles for 50°N for the same months.

below the mixed layer, which takes over a sizeable part of the mixing work in our model. For the penetrative convection, we have used the same basic value as Woods and Barkmann, namely, $f = 0.12$, but we do not allow this to decrease with h (see section 2.2).

Figure 5 takes a detailed look at the development of the temperature profiles over a year. It compares model results for 50°N to observations from ocean weather station Papa, at the same latitude. Although it is problematic to compare a single station with a zonal average, OWS Papa seemed suitable because its annual sea surface temperature cycle is close to the zonal average cycle. Papa is also known to be little affected by horizontal advection and has been used before to validate vertical mixing models [e.g., *Martin,* 1985]. A look at the monthly profiles suggests that the essence of the mixing process has been captured well by the model. The main difference is that winter mixing goes below 150 m in the model, whereas at station Papa it penetrates only to 120 m. This is related to a strong halocline at that depth [see *Tabata,* 1976, Figure 16]. Our model does not account for salinity gradients.

At this point, a discussion of the heat diffusion below the mixed layer seems appropriate. It acts as a simple parameterization for mixing processes associated with current shear, internal waves, motion along isopycnals, etc. A single value for the diffusion constant K has been used, independent of depth and latitude. *Munk* [1966] suggested $K = 1.3$ cm^2/s as a good average value, while *Craig* [1969] proposed 2 cm^2/s. More recently, *Hoffert et al.* [1980] derived $K = 0.6$ cm^2/s from radiocarbon tracer data.

We have therefore chosen to run our model simulations for two alternative values of K: 0.5 and 2.0 cm^2/s. The lower value was used for the profiles shown in Figure 5. The choice of K determines the curvature of the profiles below the mixed layer, and the month to month temperature change in this region. The strong similarity between model profiles and observations (Figure 5) cannot be reproduced with the higher value for K. The model experiments therefore suggest that in the thermocline below the mixed layer K is close to 0.5 cm^2/s. Note that this estimate of K is practically independent of the upwelling velocity w, because of the short time scales involved.

5. RESPONSE TO CLIMATIC CHANGE

The model has shown its ability to reproduce present ocean temperatures well, and the next step is to apply it to a changing climate. For this purpose we add "greenhouse radiation" to the surface forcing as discussed in section 3.1 and analyze the resulting changes in the thermal structure.

The time variation of this extra heat flux was prescribed by

$$\Delta Q(t) = \Delta Q_{2x}\, B\, t\, (ln2)^{-1}\, e^{\alpha t} \qquad (6)$$

[*Wigley and Schlesinger,* 1985]. Here $B = 5.59\times10^{-4}$ yr^{-1}, $\alpha = 8.69\times10^{-3}$ yr^{-1}, and t is the time in years after 1850. The starting point is 1850, although our equilibrium solutions are based on average climatology for the middle of this century. However, this small difference in initial condition has a negligible, second-order effect on the calculated temperature changes. ΔQ_{2x}, the greenhouse heating for CO_2 doubling, varies with latitude according to *Ramanathan et al.* [1979]. The values were taken from a table of *Schneider and Thompson* [1981] and range from 4.6 W/m^2 in low latitudes, to 3.7 W/m^2 at 50°N and 50°S.

These greenhouse simulations allow us to answer questions such as the following: How quickly does the warming penetrate into the ocean? What role does the seasonal mixed layer cycle play in this process? What is the relative importance of heat storage in the upper ocean and the deep ocean? How will the climatic warming be modified by the oceanic heat capacity? How will the warming affect the seasonal mixed layer cycle?

5.1. *Greenhouse Simulation for 40°S*

The greenhouse simulations were performed for all latitudes, starting at the equator, as described in section 3.2. The equilibrium solutions were used as initial conditions. The temperature changes are generally similar for all latitudes, differences mainly resulting from the latitude dependence of the greenhouse forcing. As an example, we show the results for 40°S.

Figure 6 illustrates how the ocean balances the additional flux of greenhouse radiation. It can do this by radiating heat into space, by advecting it poleward, or by using it to heat up (storage term). The upper curve shows the greenhouse radiation as prescribed by (6), starting with 0 in 1850. The shaded areas show the proportions of this which are radiated back, advected poleward, stored in the top 250 m, or used to heat the water below 250 m. Figure 6 shows that the heat penetrating below 250 m is a significant proportion of the total. The deep ocean cannot be neglected; climate models that only account for the surface layer of the ocean will be inaccurate.

The size of the combined storage terms shows us how far from equilibrium the system is. In equilibrium they will vanish. When advection and back radiation balance only half the incoming flux, then this means that only about half the equilibrium warming has occurred. The disequilibrium ratio, $\Delta T/\Delta T_{eq}$, is 65 % for $K = 0.5$ cm^2/s and 45% for

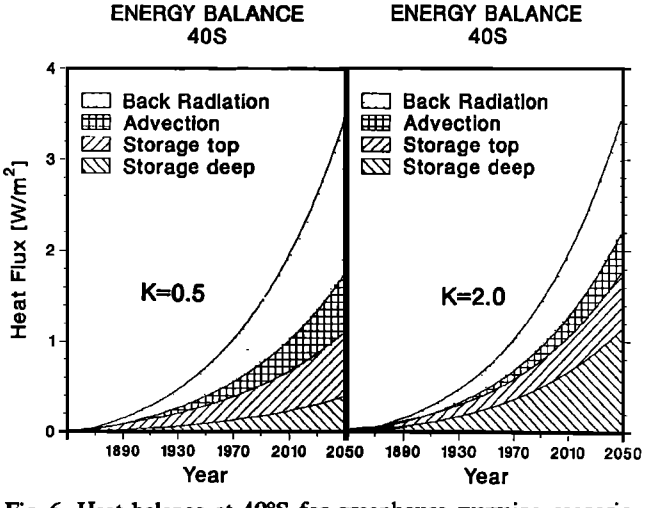

Fig. 6. Heat balance at 40°S for greenhouse warming scenario, with (left) $K = 0.5$ cm^2/s, and (right) $K = 2.0$ cm^2/s. The increase in back radiation and advection (relative to the equilibrium solution) as well as storage above and below 250 m are shown. Added together, these fluxes equal the greenhouse heating.

$K = 2.0$ cm^2/s. We can also work out how many years it will take until the actual warming reaches the equilibrium warming for a given year. This time lag is a measure of how the ocean's heat capacity slows down global warming. It depends strongly on the amount of mixing in the deeper water. For $K = 0.5$ cm^2/s the time lag is 27 years, and for $K = 2.0$ cm^2/s it is 47 years (for 1990).

The temperature increase associated with the heat fluxes of Figure 6 is shown in Figure 7. This temperature rise depends on the delay discussed above: the surface temperature increases faster if there is less mixing. The surface temperature increase calculated for the period from 1850 to 1990 is 0.8° or 0.6°C, respectively. The lower value is consistent with the observed 0.5°C change in air temperature over the past 100 years [*Jones et al.*, 1986].

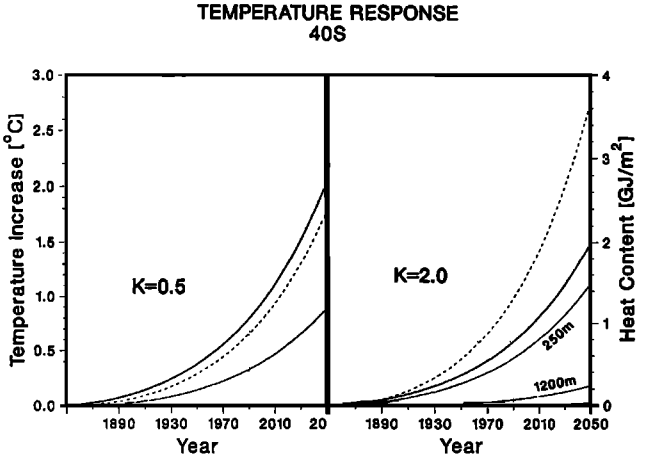

Fig. 7. Temperature response for the simulations shown in Figure 6. The heavy curve is the sea surface temperature increase. The curves below it are the temperature rise at 250, 1200, and 2100 m depth. The dashed curve is the integrated heat content of the water column relative to the year 1850 (scale on the right).

This result shows that the ocean's thermal inertia can slow down the warming, to the extent that an equilibrium rise of 3°C for CO_2 doubling becomes consistent with the observed temperature rise. It should be noted, however, that the observed temperatures are the result of a combination of several external forcings (e.g., volcanic, solar cycles, aerosol pollution, CO_2). A model that accounts only for the effect of CO_2 increase can therefore not easily be compared to observations [*Gilliland*, 1982].

Figure 7 also shows the total heat content of the water column. Not surprisingly, this increases faster in the case of more mixing, in spite of the cooler surface temperature. The distribution of the heat with depth is shown in Figure 8.

The results presented so far agree well with those from box-advection-diffusion (BAD) models which have a fixed mixed layer box instead of the variable mixed layer depth of our model [e.g., *Cess and Goldenberg*, 1981; *Wigley and Schlesinger*, 1985; *Wigley and Raper*, 1987]. Cess and Goldenberg predict a shorter time lag (20 years), but this seems to be due to a different surface forcing, rather then differences in the ocean model. Their greenhouse

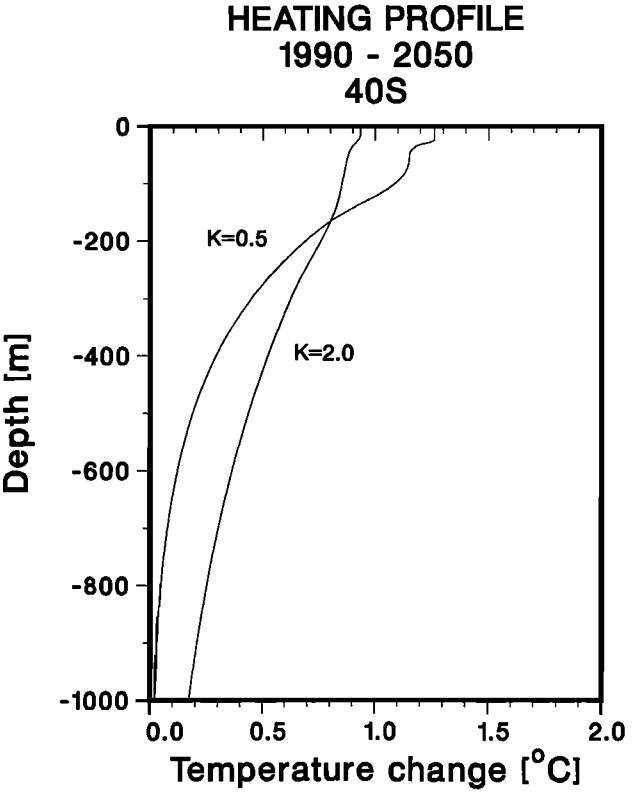

Fig. 8. Temperature increase between 1990 and 2050, as it depends on depth for $K = 0.5$ cm^2/s and $K = 2.0$ cm^2/s.

radiation reaches 4 W/m^2 as early as 2025, thus leading to a faster warming.

Henderson-Sellers [1987, p.357] explains the much smaller temperature rise in his model, by saying that "the convective dynamics of an ocean with a seasonal cycle contribute an ameliorative effect on increasing oceanic surface temperatures." The results of our model, which includes a realistic seasonal cycle and convection, do not support this interpretation. We will have a closer look at the effects of the seasonal cycle below.

5.2. *The Oceanic Mixed Layer*

The seasonal cycle of mixed layer depth and temperature is shown in Figure 9, both for the equilibrium solution and the simulation for the year 2050. No seasonal variation in the greenhouse forcing was used, and the temperature increase is nearly uniform over the whole year.

The behavior of the mixed layer depth is very different. We see the familiar cycle of gradual deepening through autumn and winter and sudden formation of a shallow warm surface layer in spring. During most of the year, the mixed layer depth is hardly affected by the climate warming. But in winter the maximum depth is reduced by about 30 m in the warmer climate. This may have an effect on the biota. For example, reduced depth of winter convection could mean that less nutrients are available in the surface waters in spring. Figure 9 shows a simulation for 50°S; in lower latitudes the change in winter mixing is smaller. The reduction of mixed layer depth contradicts earlier model results of *Hunt and Wells* [1979], who

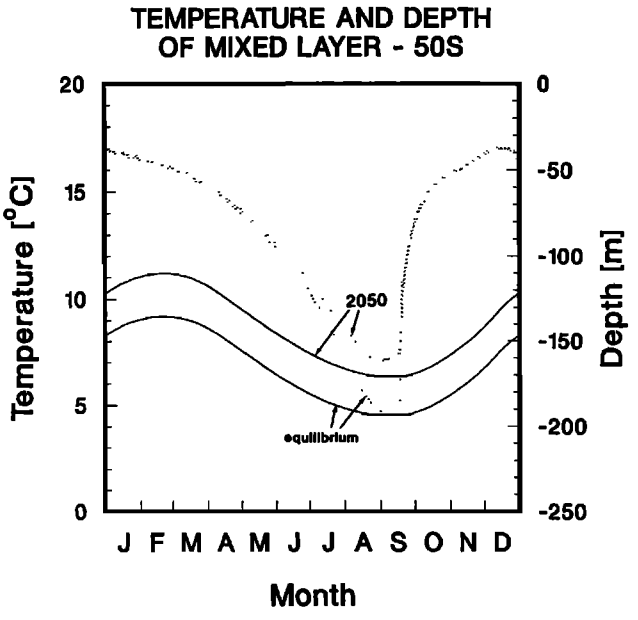

Fig. 9. Seasonal cycle of mixed layer temperature (solid curve) and depth (dotted curve) at 50°S. The bottom curves are the equilibrium solution; the top curves are modelled for the year 2050.

obtained an increase of winter mixing depth for CO_2 doubling.

We can also ask the reverse question to the above: how does the seasonal mixed layer cycle affect the heat uptake by the ocean on climatic time scales? A comparison run with a fixed mixed layer depth of 60 m was performed, all other model aspects remaining the same. The difference in the monthly temperature profiles (Figure 10) is striking, and it is quite plausible that this could have an important effect on the downward heat transport in a warming climate. To check this, we plotted the temperature increase from 1990 to 2050 versus depth for both cases (Figure 11). We can see that the deep winter mixing acts to pump more heat into depths between 100 m and 200 m. This leads to a faster downward diffusion of heat, compared to the fixed mixed layer case. The difference is, however, small compared to the present overall uncertainty of climate predictions.

5.3. *Changes in Wind and Upwelling*

So far, we have only considered the effects of temperature changes resulting from a change in radiation budget. However, other factors, like the intensity of atmospheric and oceanic circulation, could also change in a changing climate. First, we consider the effect of a possible change in wind speed. Global circulation models predict a greater warming near the poles and thus a reduced temperature gradient between poles and low latitudes. This makes a reduction in the strength of the westerlies near 50°S plausible. To test the sensitivity of the oceanic mixed layer to a wind change, we ran a simulation with a gradual (linear) decline of average wind speed by 10% between 1990 and 2050. This wind change in our model led to a reduction of the mixed layer depth throughout the year. By the year 2050, when the wind was 10% less, the average mixed layer depth had declined by 11 m, compared to 6 m in a simulation with unchanged wind. Heat transport to deeper waters was slightly reduced.

Another possible effect of climatic change, mentioned in section 3.2, is a decline or even collapse of the thermohaline circulation as a result of warming near the poles. Widespread melting of ice could reduce the surface salinity in the sinking areas and thus contribute to a reduction of deepwater formation. *Mikolajewicz et al.* [1990] have recently published results from the Hamburg ocean general circulation model, where greenhouse warming leads to a reduction of the deep water formation rate by one third after 40 years, because of reduced surface salinity.

In our model, a reduced deep circulation means a

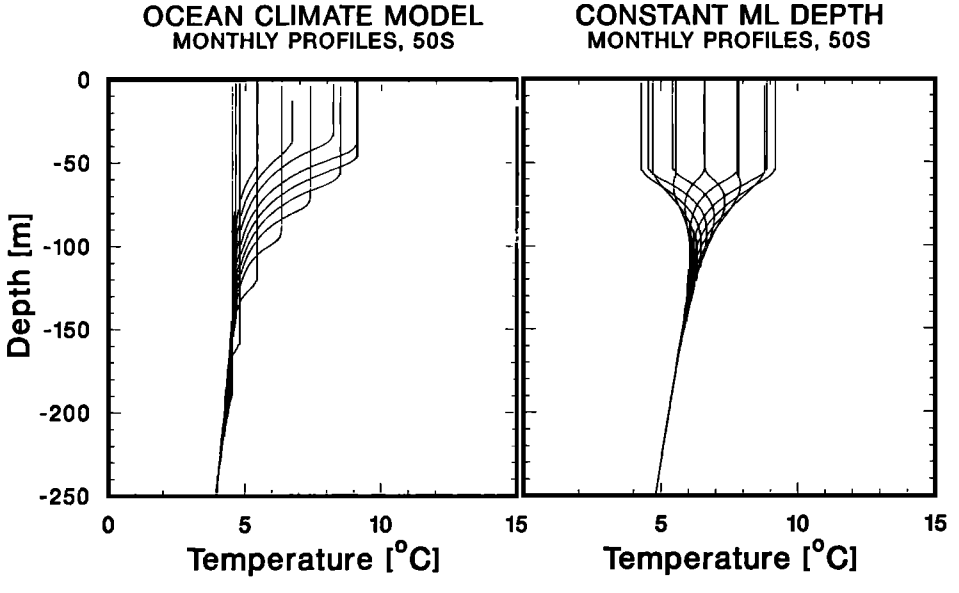

Fig. 10. (Left) monthly temperature profiles for the full model and (right) for a version with constant mixed layer depth.

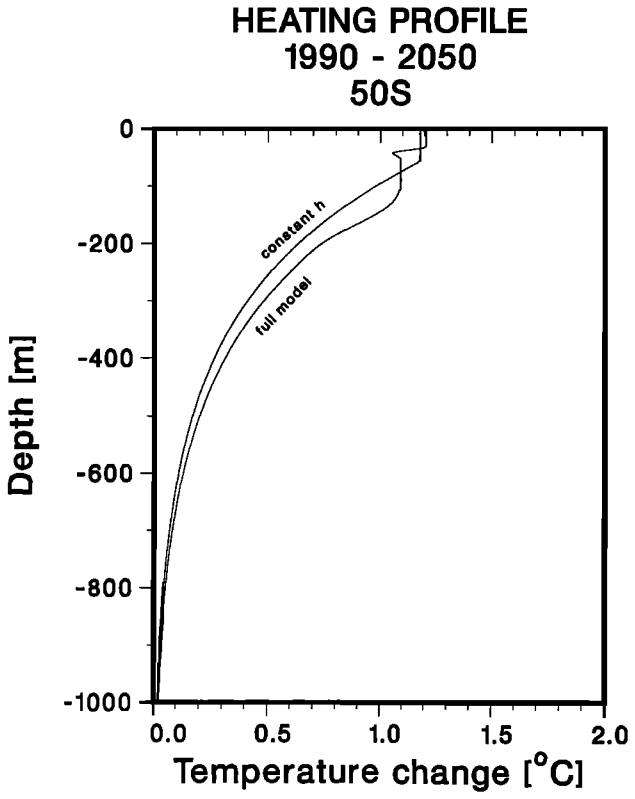

Fig. 11. Temperature rise as it depends on depth for the two cases shown in Figure 10. The full model shows a slightly greater temperature increase.

reduction of the upwelling velocity w. To examine the sensitivity of our model to such a change, we performed a simulation where w decreased linearly to zero between 1990 and 2030. Results for this scenario show a greatly enhanced heat uptake by the deep ocean, in agreement with predictions from the three-dimensional model of *Bryan and Spelman* [1985]. Surface temperatures rise sharply in low latitudes and decline in high latitudes, due to a reduction in poleward heat transport. The latter effect could, however, be at least partly cancelled by adjustments in atmospheric heat transport, which we cannot account for in our model.

Watts and Morantine [1990] have used a similar model (however, not including mixed layer physics) to simulate the effect of a sudden "switch-off" of the global thermohaline circulation. They obtain a sharp transient temperature drop at all latitudes, before the low latitudes approach their new warmer equilibrium temperature. For a sudden end to deepwater formation we obtained the same result. The more gradual decline of w over 40 years, however, prevents the transient temperature drop at low latitudes.

All three models (Mikolajewicz et al., Watts and Morantine, and our model) agree that reduced deepwater formation would lead to cooling at high latitudes, particularly in the regions of sinking. This effect can counteract the ice albedo feedback, which enhances the temperature rise at high latitudes in atmospheric general circulation models. None of the three ocean models takes account of the atmospheric response that may result from the surface cooling in these areas. Note that the cooling constitutes a stabilizing feedback on the deepwater formation rate, so that a complete collapse of the thermohaline circulation is unlikely.

In spite of the uncertainty that still surrounds this issue, it seems very likely that the total heat uptake by the ocean is very sensitive to changes in the thermohaline circulation. A decline in this circulation could greatly increase the thermal expansion component of sea level rise. This adds uncertainty to estimates of thermal expansion which are based entirely on past circulation rates. A decline in deepwater formation will also counteract high-latitude warming to some extent, which needs to be considered when looking for the greenhouse signal in observations.

5.4. *A Scenario With Constant Greenhouse Gases*

Some of the political discussion about the greenhouse effect has focused on whether to adapt to it or whether to try to prevent the worst. The argument has been raised that preventative measures would have little effect over the next decades, because of the thermal inertia of the oceans. This would lead to further warming, even if carbon emissions were cut drastically now. Our model can be used to estimate the magnitude of this effect.

For this purpose, we used a simple scenario where the greenhouse radiation increased from 1850 to 1990 as in the previous simulations but was held constant at the 1990 level from there. If recent models for the airborne carbon fraction are correct [*Harvey*, 1989], a 50% reduction in CO_2 emissions would be sufficient to stabilise the carbon content of the atmosphere. This could be achieved very quickly through increased energy efficiency, a halt to deforestation, and a vigorous forest planting program [*Woodwell*, 1989].

The results for this scenario are shown in Figure 12 for $K = 2.0$ cm^2/s. The warming continues due to the thermal flywheel effect of the ocean, but it is slowed down dramatically. The calculated temperature rise from 1990 to 2050 is only 0.24°C, compared to 0.91°C in the "do nothing" case. A slow warming continues for centuries, until a new equilibrium is reached at 0.68°C warmer than 1990. (For $K = 0.5$ cm^2/s, the warming from 1990 to 2050 is also 0.24°C. The new equilibrium is only 0.45°C warmer than 1990, because in this case we would already be closer to the equilibrium warming for present carbon levels.)

The slow approach to equilibrium is a result of the continued heat uptake by the deep ocean, which takes a very long time to equilibrate with the warmer surface temperature. We can see this in the total heat content curve in Figure 12 (dashed curve), which does not level off as quickly as the surface temperature. The disequilibrium ratio of the heat content is at present only 20%. This means that by stabilizing the carbon content of the atmosphere we can slow down further surface warming considerably within years. We would still be committed, however, to an unavoidable sea level rise from thermal expansion, which would be 4 times larger than the greenhouse expansion to date. It is interesting to note that the deep ocean can act as a memory for warming events. Even a temporary surface warming leaves a heat signal that slowly spreads through the deep ocean, leading to thermal expansion that is irreversible for centuries.

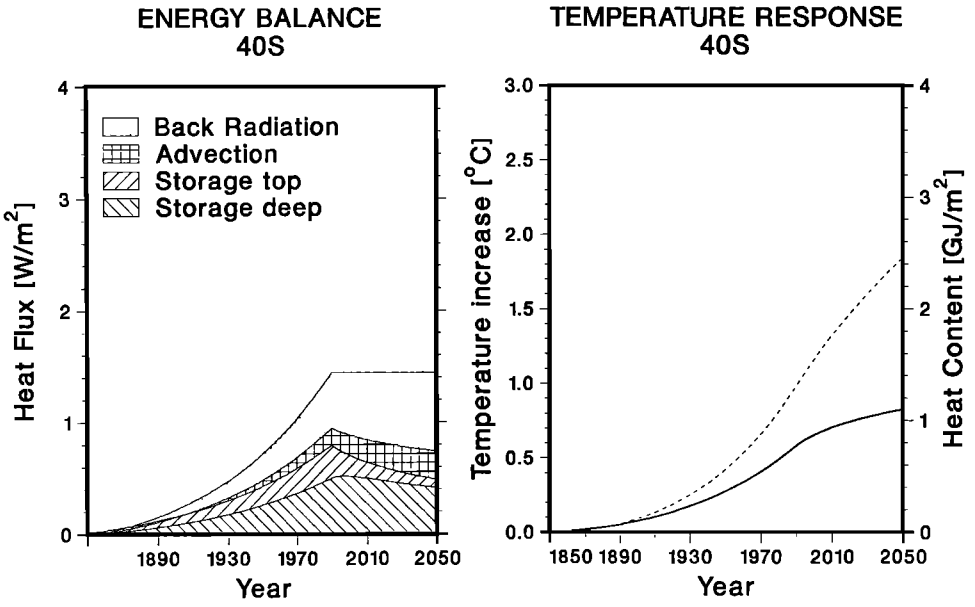

Fig. 12 Results for a simulation with constant greenhouse radiation after 1990, for 40°S and $K = 2.0$ cm²/s.

6. Conclusion

The success of our ocean model in simulating present-day conditions gives credence to its application to the greenhouse effect. Although the limitations of the model do not allow stand-alone predictions of climatic change, the model is able to answer questions about the role of the oceans in a warming climate. It is also suitable as a process model for vertical mixing, which can be included in a more comprehensive climate model.

For an equilibrium warming of 3°C for CO_2 doubling, the transient response of ocean temperatures was analyzed. The expected warming from 1850 to 1990 was found to be between 0.5° and 0.8°C, reaching between 1.5° and 2°C by 2050. These values correspond to a time lag of 27-47 years, depending on the intensity of mixing in the deeper waters, due to the oceanic heat capacity. Both the top 250 m of the ocean and the deeper waters play an important part in this buffer effect.

This warming would reduce the depth of mixing in the surface waters of the higher latitudes in winter, when it is governed by convection. The summer mixed layer depth, in contrast, is determined primarily by wind mixing and is sensitive to possible changes in wind speed.

The seasonal cycle of mixed layer depth acts to pump the heating signal down into the deep ocean, but the difference to a fixed mixed layer depth model is not large. An uncertain factor in climate predictions is the global thermohaline circulation. It is plausible that a warming of the surface waters could have a strong effect on this circulation. The model experiments suggest that this would have a major impact on heat uptake by the ocean.

Finally, a test scenario has shown that a reduction in greenhouse gas emissions would slow down the climatic warming considerably, in spite of the thermal flywheel effect of the ocean. But the longer humankind waits before action is taken, the more we commit ourselves to further warming and long-term sea level rise.

Acknowledgment. I am grateful to Dulcie Smart, who made many suggestions that improved the clarity of the paper.

References

Bryan, K., and M. J. Spelman, The ocean's response to a CO_2 induced warming, *J. Phys. Oceanogr., 90*, 11,679-11,688, 1985.

Bryan, K., S. Manabe, and M. J. Spelman, Interhemispheric asymmetry in the transient response of a coupled ocean-atmosphere model to a CO_2 forcing, *J. Phys. Oceanogr., 18*, 851-867, 1988.

Cess, R. D., and S. D. Goldenberg, The effect of ocean heat capacity upon global warming due to increasing atmospheric CO_2, *J. Geophys. Res., 86*, 498-502, 1981.

Craig, H., Abyssal carbon and radiocarbon in the Pacific, *J. Geophys. Res., 74*, 5491-5506, 1969.

Garwood, R., An oceanic mixed layer model capable of simulating cyclic states, *J. Phys. Oceanogr., 7*, 455-468, 1977.

Gaspar, P., Modeling the seasonal cycle of the upper ocean, *J. Phys. Oceanogr., 18*, 161-180, 1988.

Gill, A. E., and J. S. Turner, A comparison of seasonal thermocline models with observations, *Deep Sea Res., 23*, 391-401, 1976.

Gilliland, R. L., Solar, volcanic and CO_2 forcing of recent climatic changes, *Clim. Change, 4*, 111-131, 1982.

Harvey, L. D. D., Managing atmospheric CO_2, *Clim. Change, 15*, 343-381, 1989.

Harvey, L. D. D., and S. H. Schneider, Transient climate response to external forcing on 10^0 to 10^4 year time scales, 1, *J. Geophys. Res., 90*, 2191-2205, 1985.

Henderson-Sellers, B., Modeling SST rise resulting from increasing atmospheric carbon dioxide concentrations, *Clim. Change, 11*, 349-359, 1987.

Henderson-Sellers, B., Embedding stratification models in ocean general circulation climate models, in *Small-Scale Turbulence and Mixing in the Ocean*, edited by J. C. Nihoul and B. Jamart, pp. 95-108, Elsevier, New York, 1988.

Hoffert, M. I., A. J. Callegari, and C. T. Hsieh, The role of deep sea heat storage in the secular response to climatic forcing, *J. Geophys. Res., 85*, 6667-6679, 1980.

Hsiung, J., Estimates of global oceanic meridional heat flux, *J. Phys. Oceanogr., 15*, 1405-1413, 1985.

Hunt, B. G., and N. G. Wells, An assessment of the possible future climatic impact of CO_2, *J. Geophys. Res., 84*, 787-791, 1979.

Jones, P. D., T. M. L. Wigley, and P. B. Wright, Global temperature variations between 1861 and 1984, *Nature, 322*, 430-434, 1986.

Kraus, E. B., and J. S. Turner, A one-dimensional model of the seasonal thermocline, *Tellus, 19*, 98-105, 1967.

Luyten, J. R., J. Pedlosky, and H. Stommel, The ventilated thermocline, *J. Phys. Oceanogr., 13*, 292-309, 1983.

Martin, P. J., Simulation of the mixed layer at OWS November and Papa with several models, *J. Geophys. Res., 90*, 903-916, 1985.

Meehl, G. A., A calculation of ocean heat storage and effective ocean surface layer depths for the northern hemisphere, *J. Phys. Oceanogr., 14*, 1747-1761, 1984.

Mikolajewicz, U., B. D. Santer, and E. Maier-Reimer, Ocean response to greenhouse warming, *Nature, 345*, 589-593, 1990.

Munk, W. H., Abyssal recipes, *Deep Sea Res., 13*, 707-736, 1966.

Niiler, P. P., and E. B. Kraus, One-dimensional models of the upper ocean, in *Modelling and Prediction of the Upper Layers of the Ocean*, edited by E. B. Kraus, pp. 143-172, Pergamon, New York, 1977.

Paulson, C. A., and J. J. Simpson, Irradiance measurements in the upper ocean, *J. Phys. Oceanogr., 7*, 952-956, 1977.

Ramanathan, V., M. S. Lian, and R. D. Cess, Increased atmospheric CO_2: Zonal and seasonal estimates of the effect on the radiation energy balance and surface temperature, *J. Geophys. Res., 84*, 4949-4958, 1979.

Schneider, S. H., and S. L. Thompson, Atmospheric CO_2 and climate: Importance of the transient response, *J. Geophys. Res., 86*, 3135-3147, 1981.

Tabata, S., The general circulation of the Pacific Ocean and a brief account of the oceanographic structure of the North Pacific, *Atmosphere, 14*, 1-27, 1976.

Thompson, S. L., and S. H. Schneider, A seasonal zonal energy balance climate model with an interactive lower layer, *J. Geophys. Res., 84*, 2401-2414, 1979.

U.S. Navy, Marine climatological atlas of the world, vol. IX, *NAVAIR Doc. 50-1C-65*, Washington, 1981.

Watts, R. G., and M. Morantine, Rapid climate change and the deep ocean, *Clim. Change, 16*, 83-97, 1990.

Wigley, T. M. L., and S. C. B. Raper, Thermal expansion of sea water associated with global warming, *Nature, 330*, 127-131, 1987.

Wigley, T. M. L., and M. E. Schlesinger, Analytical solution for the effect of increasing CO_2 on global mean temperature, *Nature, 315*, 649-652, 1985.

Woods, J. D., and W. Barkmann, The response of the upper ocean to solar heating, I, The mixed layer, *Q. J. R. Meteorol. Soc., 112*, 1-27, 1986.

Woodwell, G. M., The warming of the industrialised middle latitudes 1985-2050: Causes and consequences, *Clim. Change, 15*, 31-50, 1989.

S. Rahmstorf, Research School of Earth Sciences, Victoria University, P.O. Box 600, Wellington, New Zealand.

(Received May 7, 1990;
revised August 22, 1990;
accepted September 21, 1990.)